Elastic relaxation in an ultrathin strained silicon-on-insulator structure

Gang Xiong,[1,a)] Oussama Moutanabbir,[2,b)] Xiaojing Huang,[1,3] Seyed A. Paknejad,[1] Xiaowen Shi,[1] Ross Harder,[3] Manfred Reiche,[2] and Ian K. Robinson[1,4]
[1]*London Centre for Nanotechnology, University College London, London WC1H 0AH, United Kingdom*
[2]*Max Planck Institute of Microstructure Physics, Weinberg 2, 06120 Halle (Saale), Germany*
[3]*Advanced Photon Source, Argonne, Illinois 60439, USA*
[4]*Research Complex, Harwell-Oxford Campus, Didcot OX11 0DE, United Kingdom*

(Received 17 June 2011; accepted 21 August 2011; published online 16 September 2011)

Coherent x-ray diffraction was used to study the relaxation in single ultrathin strained silicon structures with nanoscale accuracy. The investigated structure was patterned from 20 nm thick strained silicon-on-insulator substrate with an initial biaxial tensile strain of 0.6%. Two-dimensional maps of the post-patterning relaxation were obtained for single 1×1 μm^2 structures. We found that the relaxation is localized near the edges, which undergo a significant contraction due to the formation of free surfaces. The relaxation extent decreases exponentially towards the center with a decay length of 50 nm. Three-dimensional simulations confirmed that over-etching is needed to explain the relaxation behavior. © *2011 American Institute of Physics*. [doi:10.1063/1.3637634]

In nanoscale semiconductor systems, functionalities can be achieved by controlled manipulation of strain.[1,2] For example, strain engineering has been used in modern semiconductor industry to improve charge carriers transport since the 65 nm technology node of metal oxide semiconductor field effect transistors (MOSFETs). Introducing strain in silicon can modify its band structure and lead to charge carriers mobility enhancement. Indeed, nearly two times electron mobility increase was recently demonstrated for tensile strained Si channel *n*-MOSFETs.[3] This has sparked interest in developing processes for strain control in Si devices and nanostructures. With recent progress in direct wafer bonding and thin layer transfer techniques,[4,5] tensile strained Si can be grown on a relaxed SiGe and transferred onto a SiO_2-capped Si wafer achieving the strained Si-on-insulator (SSOI) substrate. SSOI combines the advantages of Si-on-insulator technology[6] with that of strained Si.[1] However, the effective strain in semiconductor structures can be drastically altered due to the integration process, thermal annealing, and particularly the active region patterning. There is strong motivation to understand the fundamental properties of strained Si structures during the different steps of processing, which requires accurate probe of the local strain.

Recent progress in probing the strain distribution in nanostructures includes utilizing Raman spectroscopy,[7,8] transmission electron microscopy (TEM) based techniques,[9] and x-ray diffraction based techniques, such as microbeam x-ray diffraction,[10] high resolution x-ray diffraction,[11,12] and grazing incidence x-ray diffraction (GIXRD).[13] Raman spectroscopy provides a fairly good spatial resolution and does not require a specific sample preparation, but it is limited to bare Si structures as the top metallic layer in the device prohibits the laser penetration. Latest TEM-based techniques, such as nanobeam diffraction and dark-field holography, claim sub-10 nm resolution in strain mapping.[14] Nevertheless, the major limitation of these techniques has to do with the relaxation during TEM specimen preparation, which results in uncertainties in strain analysis. High resolution x-ray diffraction and GIXRD allow characterizing the strain without special sample preparation. However, as the beam footprint on the sample is in millimeter scale, those techniques integrate the reflection intensities of a number of structures. It was argued that very small deviations from ideal periodicity cause the smearing out of any ultrafine fringes.[12]

In this paper, we demonstrate that the strain in individual ultrathin SSOI structures can be visualized with a high spatial resolution by using the recently developed coherent x-ray diffraction (CXD) method. The post-patterning structures present an elastic relaxation with exponential attenuation from the edges into the center of the structure. Three-dimensional (3D) finite element analysis (FEA) was performed to gain more insight into the complexity of this relaxation phenomenon and compared with the experiment result.

SSOI wafers consisting of ultrathin strained Si film with a thickness of 20 nm were used in this study. The strained Si film was epitaxially grown on a $Si_{0.84}Ge_{0.16}$ layer and capped by a ~200 nm-thick SiO_2 layer. Using direct wafer bonding and ion-cut process,[4,5] the strained Si layer was then transferred onto a Si wafer. The transferred layer is under a biaxial tensile strain of 0.6% as confirmed by Raman spectroscopy. An ordered array (20×20) of square elements with a lateral dimension of 1 μm, separated by 100 μm both horizontally and vertically, was patterned on a negative resist using electron-beam lithography. Reactive ion etching (RIE) was applied to transfer the pattern to the strained layer, leading to array of square strained Si structures on oxide. The patterned islands are aligned along the $\langle 110 \rangle$ direction. The etching was performed at $-60\,^{\circ}C$ using a mixture of SF_6 (100 sccm) and O_2 (5 sccm) with a relatively low power of 40 W. Here, the chemical reactivity is dominant. High resolution XTEM investigations (not shown here) confirmed the absence of any damage at the formed edges. Figure 1(a) displays a typical atomic force microscopy (AFM) image of the investigated structures. The square has a lateral size of 950×950 nm^2 slightly below 1×1 μm^2, indicating a small

a)Electronic mail: g.xiong@ucl.ac.uk.
b)Electronic mail: moutanab@mpi-halle.mpg.de.

 © 2011 American Institute of Physics

Author complimentary copy. Redistribution subject to AIP license or copyright, see http://apl.aip.org/apl/copyright.jsp

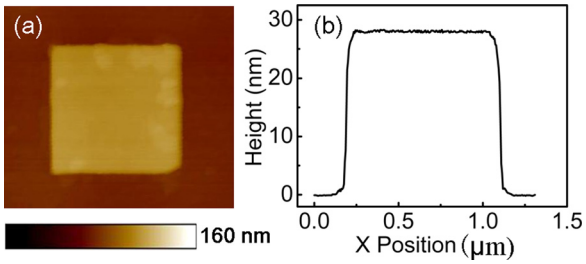

FIG. 1. (Color online) (a) AFM image of a 20 nm thick ~1 μm × 1 μm strained Si structure and (b) the height profile across the center of the structure.

shrinkage of the transferred pattern. This could be due to lateral etching during the RIE processing. Figure 1(b) is the cross section profile of the structure showing that the island has a height of 28 nm, which means the etching has gone deep enough to cut through the 20 nm thick Si layer and ensured that every square is an isolated structure.

The CXD experiments were performed at the Advanced Photon Source, Argonne National Laboratory, Beamline 34-ID-C. A 9 keV coherent x-ray beam was focused to about 1.5 μm with Kirkpatrick-Baez mirrors and is used to illuminate a single patterned structure. During the measurements, by rotating the sample, diffraction patterns were measured for the rocking curve of the (−111) Bragg reflection. A CCD detector with 20.0 μm pixel size was used to collect the 2D diffraction slice for each rotation angle. Stacking these 2D frames together gives a full 3D diffraction pattern.

The scattered amplitude is a complex quantity, $A = |A|\exp(i\varphi)$, and by inverting the measured amplitude back to direct space using phase retrieval algorithms, one can obtain the complex three dimensional electron density of the sample. Detailed reconstruction procedures have been reported earlier,[15–17] which recover the "lost phase" by oversampling the reflection intensity distribution. In direct space, the reconstructed phase (φ) of the complex density describes the displacement of the crystal planes parallel to the Q-vector, $\varphi = \boldsymbol{Q}.\boldsymbol{r}$. This method can provide quantitative phase information which is sensitive to lattice distortions.

Fig. 2(a) shows the diffraction pattern from a single SSOI square structure viewed along the x direction. The asymmetrical shape is a typical characteristic when the investigated structure is strained. The pattern was inverted using a Fienup's Hybrid Input-Output phase retrieval algorithm with a rectangular prism-shaped support and a [$-\pi/2$, $\pi/2$] phase constraint.[16] Figs. 2(b) and 2(c) are the reconstructed magnitude and phase of the square structure. Here, a phase of 2π represents a rigid body displacement equal to the lattice parameter in the {−111} direction, which is 0.3135 nm. The magnitude shows that the structure has a lateral size of 930 × 940 nm, consistent with the AFM measurement. The phase map shown in Fig. 2(c) represents the displacement along the Q-vector direction, which is aligned with the horizontal edges of the square for the (−111) reflection. It can be seen that there are two strong phase stripes near the left and right edges, and the corresponding displacements are relatively compressive and point to the centre. The fact that the edges are contracted is attributed to the formation of free surfaces from the RIE patterning leading to relaxation of the

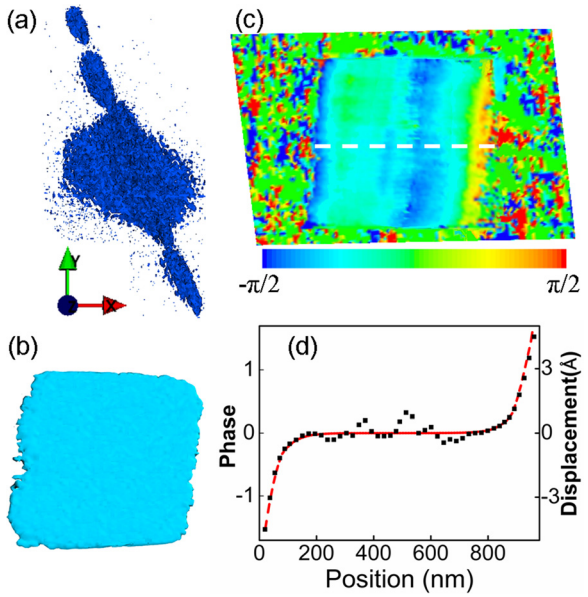

FIG. 2. (Color online) The 3D diffraction pattern (view along the z direction) from (−111) plane of a strained Si square structure (a), the reconstructed amplitude (b), phase (c), and a cross section plot of the phase variation along the x direction (black square), with the COMSOL simulated displacement (red dashed line) (d).

initial tensile strain in the film. The relaxation is pronounced in the region within ~150 nm from the edges and rapidly attenuates towards the center where the initial strain is preserved. This is in qualitative agreement with an earlier Raman study.[8] However, in that work, the limited resolution prevents the observation of the exact nature of strain in the region near the edges. According to Rayleigh wave solution of the continuum elasticity equation, a distortion should die off exponentially inside the solid from a surface.[18] To examine the strain decay behavior, we extracted the phase along the dotted line in Fig. 2(c) and the result is shown in Fig. 2(d). It can be seen that the phase change does follow an exponential decay, and by fitting the experimental data, the decay length can be derived, which is 50 ± 15 nm for the present sample. Apart from Rayleigh wave equations, there are other possible models to explain this behavior. For example, the "shear-lag" approximation predicts a hyperbolic cosine dependence on stress with respect to distance which will also display an exponential decay near the edges.[10] Fig. 2(d) also shows that there are some positions in the film where the phases deviate from the base line; this may due to the presence of dislocations in the film from the epitaxial growth of strained Si on SiGe.

In order to gain more insight into the relaxation phenomenon, we performed detailed 3D FEA using the COMSOL software. Fig. 3(a) is the schematic side view of the modeled system. It consists of a 20 nm thick L × L Si square on top of a 1 μm thick SiO_2 layer and an additional thickness d of SiO_2 underneath the structure to account for possible over-etching from the RIE process. Without over-etching, the model predicts a too short relaxation decay length. Manual optimization of the model yielded L = 940 ± 20 nm and d = 9 ± 4 nm. Here, we do not consider any irregularity (e.g., roughness) in the patterned structures. Both materials are linearly elastic in the calculations. An initial tensile strain

Author complimentary copy. Redistribution subject to AIP license or copyright, see http://apl.aip.org/apl/copyright.jsp

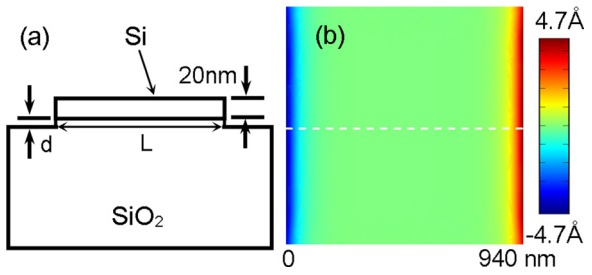

FIG. 3. (Color online) Schematic side view (not to scale) of the modeling system (a) and the simulated in-plane displacement in the x direction (b).

of 0.6% was applied to the Si layer. The relaxation phenomenon was then simulated by taking away the constraints at the free facets and allowing the system to achieve equilibrium.

Fig. 3(b) shows the simulated in-plane displacement component along the x direction for $L = 940$ nm and $d = 9$ nm. It can be seen that the relaxations are pronounced near the edges of the square, in agreement with our CXD experiment results. To compare with the experimentally measured phase changes, the displacements along the dotted line in Fig. 3(b) are extracted and superposed in Fig. 2(d) (red dashed line). It can be seen that they have very similar decay behaviors. The simulated displacement indeed follows an exponential decay from the edge and the fitted decay length is 45 nm, reasonably consistent with the experiment results. As the theoretical modeling agrees with the experimental data, the effect of RIE damage on the crystal is not detected, which is consistent with the XTEM observation. This result confirms the ability of CXD to probe on the nanoscale, the local strain, as well as the morphological subtleties in semiconductor devices.

In conclusion, we studied the in-plane elastic relaxation behavior of single ultrathin strained structures processed from a 20 nm thick SSOI substrate, by using the coherent-x-ray-diffraction method. Reconstruction from the (−111) diffraction pattern reveals an exponential decay of the in plane relaxation from the edge to the center, with a decay length of 50 nm, as a result of free surfaces induced by the patterning process. 3D finite element modeling confirmed this decay behavior once over-etching was allowed for. This phenomenon should be taken into consideration in the design and fabrication of SSOI-based devices.

This project is supported by the European Research Council as an FP7 Advanced grant "Nanosculpture," code 227711. APS beamline 34-ID-C was built with US national Science Foundation Grant No. DMR-9724294 and operated by the US Department of Energy, Office of Basic Energy Sciences, under Contract No. DE-AC02-06CH11357. The work at MPI-Halle was supported in part by the German Federal Ministry of Education and Research in the framework of the DECISIF project (Contract No. 13 N 9881), in part under the nanoSTRESS project, and in part under the EU network of excellence "Nanosil." The authors thank U. Doss and W. Erfurth for their technical assistance.

[1]M. Chu, Y. Sun, U. Aghoram, and S. E. Thompson, Annu. Rev. Mater. Res. **39**, 203 (2009).
[2]M. L. Lee, E. A. Fitzgerald, M. T. Bulsara, and A. Lochtefeld, J. Appl. Phys. **97**, 011101 (2005).
[3]S. Baudot, F. Andrieu, O. Faynot, and J. Eymery, Solid-State Electron. **54**, 861 (2010).
[4]O. Moutanabbir and U. Gösele, Annu. Rev. Mater. Res. **40**, 469 (2010).
[5]M. Reiche, O. Moutanabbir, C. Himcinschi, S. Christiansen, W. Erfurth, U. Gösele, S. Mantl, D. Buca, Q. T. Zhao, R. Loo, D. Nguyen, F. Muster, and M. Petzold, ECS Trans. **16**, 311 (2008).
[6]C. K. Celler and S. Cristoloveanu, J. Appl. Phys. **93**, 4955 (2003).
[7]S. C. Jain, H. E. Maes, K. Pinardi, and I. De Wolf, J. Appl. Phys. **79**, 8145 (1996).
[8]O. Moutanabbir, M. Reiche, A. Hähnel, W. Erfurth, M. Motohashi, A. Tarun, N. Hayazawa, and S. Kawata, Appl. Phys. Lett. **96**, 233105 (2010).
[9]A. Armigliato, R. Balboni, G. P. Carnevale, G. Pavia, D. Piccolo, S. Frabboni, A. Benedetti, and A. G. Cullis, Appl. Phys. Lett. **82**, 2172 (2003).
[10]C. E. Murray, H. F. Yan, I. C. Noyan, Z. Cai, and B. Lai, J. Appl. Phys. **98**, 013504 (2005).
[11]G. M. Cohen, P. M. Mooney, E. C. Jones, K. K. Chan, P. M. Solomon, and H.-S. P. Wong, Appl. Phys. Lett. **75**, 787 (1999).
[12]M. Gailhanou, A. Loubens, J.-S. Micha, B. Charlet, A. A. Minkevich, R. Fortunier, and O. Thomas, Appl. Phys. Lett. **90**, 111914 (2007).
[13]T. Baumbach and D. Lübbert, J. Phys. D **32**, 726 (1999).
[14]D. Cooper, A. Béché, J.-M. Hartmann, V. Carron, and J.-L Rouvière, Appl. Phys. Lett. **96**, 113508 (2010).
[15]I. K. Robinson and R. Harder, Nature Mater. **8**, 291 (2009).
[16]R. Harder, M. Liang, Y. Sun, Y. Xia, and I. K. Robinson, New J. Phys. **12**, 035019 (2010).
[17]G. Xiong, X. J. Huang, S. Leake, M. C. Newton, R. Harder, and I. K. Robinson, New J. Phys. **13**, 033006 (2011).
[18]L. D. Landau and E. M. Lifshitz, *Theory of Elasticity* (Pergamon, Oxford, 1986).

Author complimentary copy. Redistribution subject to AIP license or copyright, see http://apl.aip.org/apl/copyright.jsp